Clustering of vortex matter in superconductor-ferromagnet superlattices

A. A. Bespalov, A. S. Mel'Nikov, Alexandre I. Buzdin

▶ **To cite this version:**

A. A. Bespalov, A. S. Mel'Nikov, Alexandre I. Buzdin. Clustering of vortex matter in superconductor-ferromagnet superlattices. EPL - Europhysics Letters, 2015, 110 (3), pp.37003 (1-6). 10.1209/0295-5075/110/37003 . hal-01174970

HAL Id: hal-01174970
https://hal.science/hal-01174970

Submitted on 10 Jul 2015

HAL is a multi-disciplinary open access archive for the deposit and dissemination of scientific research documents, whether they are published or not. The documents may come from teaching and research institutions in France or abroad, or from public or private research centers.

L'archive ouverte pluridisciplinaire **HAL**, est destinée au dépôt et à la diffusion de documents scientifiques de niveau recherche, publiés ou non, émanant des établissements d'enseignement et de recherche français ou étrangers, des laboratoires publics ou privés.

Distributed under a Creative Commons Attribution - NonCommercial - NoDerivatives 4.0 International License

Clustering of vortex matter in superconductor-ferromagnet superlattices

A. A. Bespalov[1], A. S. Mel'nikov[2,3] and A. I. Buzdin[1]

[1] *Bordeaux University, LOMA UMR-CNRS 5798 - F-33405 Talence Cedex, France*
[2] *Institute for Physics of Microstructures, Russian Academy of Sciences 603950 Nizhny Novgorod, GSP-105, Russia*
[3] *Lobachevsky State University of Nizhny Novgorod - 23 Prospekt Gagarina, 603950, Nizhny Novgorod, Russia*

PACS 74.25.Uv – Vortex phases (includes vortex lattices, vortex liquids, and vortex glasses)
PACS 74.25.Dw – Superconductivity phase diagrams
PACS 74.20.De – Phenomenological theories (two-fluid, Ginzburg-Landau, etc.)

Abstract – Metamaterials combining superconducting (S) and ferromagnetic (F) compounds permit to attend new functionalities and reveal unusual counterintuitive effects. Here we show that SF superlattices may display a very special electrodynamics due to the nonlocal polarization of the magnetic subsystem, making the intervortex interaction *attractive* at some distances. In such superlattices the vortex matter can form an intermediate state with alternating vortex and Meissner phases. Tuning the parameters of the F and S subsystems one can engineer the phase diagram of the vortex matter. We provide concrete recommendations for the proper choice of compounds for these SF hybrid structures.

Introduction. – Abrikosov vortices and the vortex lattice are among the most curious and astonishing objects in superconductor physics. In type-I superconductors the vortex state is unstable due to the mutual attraction of vortices at all distances. On the contrary, in type-II superconductors the vortex-vortex interaction is repulsive, which results in the existence of a stable mixed state. However, for more than 40 years it has been known that such a simple classification is incomplete: even in materials with $1/\sqrt{2} < \kappa \lesssim 1$, such as pure Nb, the vortex-vortex interaction potential may become attractive at long distances [1] (certainly, this prediction is valid only at low temperatures, where the GL theory is no longer applicable). As a result, the transition from the Meissner state to the mixed state becomes a first-order phase transition: at the lower critical field H_{c1} vortices enter the superconductor at a finite concentration (see, *e.g.*, [2]). This phenomenon has been named "type-II/1 superconductivity" [2,3], as opposed to "type-II/2 superconductivity", which stands for ordinary type-II behavior.

In some cases the vortex-vortex interaction may be attractive also in high-κ superconductors. At low magnetic fields, $B \ll H_{c2}$, where H_{c2} is the upper critical field, the electrodynamics of these materials, being essentially local, is well described within the simple London theory. Therefore, the reversal of the magnetic field of a single flux line is a sufficient condition for vortex-vortex attraction [4–7]. The field reversal indeed occurs in anisotropic nonmagnetic [4–7] and magnetic [8] superconductors at certain orientations of the vortices. Then, their interaction potential is strongly anisotropic and vortices penetrate the sample in the form of separated chains [9].

In the present paper we discuss a new mechanism of vortex-vortex attraction in superconductor (S)-ferromagnet (F) superlattices. We show that the spatial dispersion of the magnetic susceptibility in ferromagnets introduces a nonlocal relation between the current density $\mathbf{j}$ and the vector potential $\mathbf{A}$. The ratio of the magnetic nonlocality scale to the superconducting length scale —the London penetration depth λ— can be changed strongly by adjusting the temperature, causing appropriate alterations in the strength of the nonlocal effects. These effects in SF superlattices can lead to a dramatic modification of all physical properties and measurable characteristics of the vortex phases: i) the vortex field and intervortex interaction potential acquire an oscillatory tail; ii) with changing temperature a *high-*κ superconductor switches from type-II/2 to type-II/1 behavior;

iii) vortex clusterization and an intermediate vortex state occur. The technological advances in the fabrication of SF superlattices (see refs. [10,11] and references therein) should permit to design a completely new type of superconducting materials with unique electrodynamical characteristics.

Basic equations. – The multilayered system under consideration is schematically shown in fig. 1. Let the magnetic layers have an easy x-axis magnetocrystalline anisotropy. In the absence of an external field we may expect the magnetization vectors to be parallel to the layers. Their mutual orientation depends on the magnetization prehistory though the minimization of the magnetostatic energy favors, of course, the configuration with opposite magnetic moments in neighboring F layers. We do not expect the particular configuration of the in-plane magnetization to cause qualitative changes in our results, so, for simplicity, we start from the ground state magnetized by the external field so that the magnetic moments in all layers are codirectional, as shown in fig. 1. We will neglect the Josephson currents between neighboring S layers, so that Josephson vortices do not appear. Such approximation is valid in the case of insulating or sufficiently thick F layers. Indeed, in the case of insulating F layers the S and F systems are electrically decoupled and the only mechanism of their interaction is the electromagnetic one. The same situation is realized in the presence of a thin oxide interlayer. When the F layer is a metal with a good electrical contact with S layers the proximity effect should play an important role [12]. However, if the thickness d_S of the S layers exceeds the superconducting coherence length ξ and the thickness of the F layers d_F exceeds the decay length of superconducting correlations in a ferromagnet (which is typically several nm), we may safely neglect the influence of the proximity effect on the superconducting properties of the SF superlattices. Then, within the London approximation the free energy of the system may be written as

$$F = \int \left[\frac{1}{8\pi\lambda_0^2} \left(\mathbf{A} + \frac{\Phi_0}{2\pi} \nabla\theta \right)^2 + \frac{K_0 \mathbf{M}_\perp^2}{2} + \frac{\alpha_0}{2} \frac{\partial \mathbf{M}}{\partial x_i} \frac{\partial \mathbf{M}}{\partial x_i} + \frac{B^2}{8\pi} - \mathbf{BM} \right] \mathrm{d}^3\mathbf{r} \tag{1}$$

(see, for example, [13]). Here, λ_0 is the London penetration depth of the superconducting layers, Φ_0 is the flux quantum, θ is the superconducting order parameter phase, $\mathbf{B} = \mathrm{rot}\,\mathbf{A}$, $\mathbf{M}$ is the magnetization, $\mathbf{M}_\perp$ is the component of $\mathbf{M}$ perpendicular to the anisotropy axis x, K_0 and α_0 are anisotropy and exchange constants, respectively. On the right-hand side of eq. (1) the first term should be integrated only over the superconducting layers, and all terms containing $\mathbf{M}$ only over the magnetic layers. If the period d of the structure is much smaller than the characteristic in-plane length scale λ_0 it is natural to average the functional over the small-scale modulation of the fields and magnetic moments at the structure period and adopt,

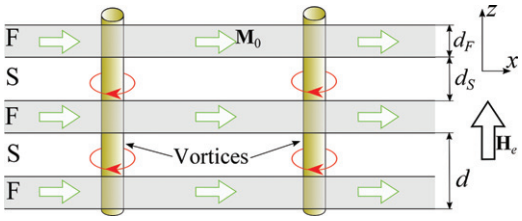

Fig. 1: (Colour on-line) Vortex lines in the SF superlattice with codirectional magnetic moments $\mathbf{M}_0$ in all layers.

thus, a standard continuous medium approximation. An external field directed along the z-axis (normal to the layers) will induce Abrikosov vortices oriented also along the z-axis and the magnetization component $\mathbf{M}_\perp$ normal to the layers. Assuming the magnitude of the full magnetization $|\mathbf{M}|$ to be fixed and the perpendicular component $\mathbf{M}_\perp$ to be small, so that $|\mathbf{M}_\perp| \ll M$, one can get the part of the free-energy functional needed to find the $\mathbf{M}_\perp$ texture and the corresponding induced magnetic fields and currents:

$$F = \int \left[\frac{1}{8\pi\lambda^2} \left(\mathbf{A} + \frac{\Phi_0}{2\pi} \nabla\theta \right)^2 + \frac{K\mathbf{m}^2}{2} + \frac{\alpha}{2} \frac{\partial \mathbf{m}}{\partial x_i} \frac{\partial \mathbf{m}}{\partial x_i} + \frac{B^2}{8\pi} - \mathbf{Bm} \right] \mathrm{d}^3\mathbf{r}, \tag{2}$$

where $\mathbf{m} = \mathbf{M}_\perp d_F/d$, $\lambda = \lambda_0\sqrt{d/d_S}$, $\alpha = \alpha_0 d/d_F$, and $K \simeq K_0 d/d_F$ is an effective anisotropy. In principle the latter value can depend, of course, on small magnetostatic corrections. In eq. (2), unlike in eq. (1), all terms are integrated over the whole sample.

Note that eq. (2) can be also derived for a bulk ferromagnetic superconductor [14–16]. Indeed, in this case the free energy of the system can be written as

$$F = \int \left[\frac{1}{8\pi\lambda^2} \left(\mathbf{A} + \frac{\Phi_0}{2\pi} \nabla\theta \right)^2 + \frac{K\mathbf{M}_\perp^2}{2} + \frac{\alpha}{2} \frac{\partial \mathbf{M}}{\partial x_i} \frac{\partial \mathbf{M}}{\partial x_i} + \frac{B^2}{8\pi} - \mathbf{BM} - \frac{\mathbf{H}_e \mathbf{B}}{4\pi} \right] \mathrm{d}^3\mathbf{r}, \tag{3}$$

where $\mathbf{H}_e$ is an external field, and all terms are integrated over the whole sample. Let us substitute in eq. (3)

$$\mathbf{M} = \mathbf{M}_0 \sqrt{1 - \frac{m^2}{M^2}} + \mathbf{m},$$

where $\mathbf{M}_0$ is a uniform magnetization directed along the easy axis x, and $\mathbf{m}$ is perpendicular to $\mathbf{M}_0$. Assuming $|\mathbf{m}| \ll M$, we obtain

$$F = \int \left[\frac{1}{8\pi\lambda^2} \left(\mathbf{A} + \frac{\Phi_0}{2\pi} \nabla\theta \right)^2 + \frac{B^2}{8\pi} + \frac{B_x m^2}{2M} - \mathbf{Bm} + \frac{\alpha}{2} \frac{\partial \mathbf{m}}{\partial x_i} \frac{\partial \mathbf{m}}{\partial x_i} + \frac{K\mathbf{m}^2}{2} - \frac{\mathbf{B}(\mathbf{H}_e + 4\pi\mathbf{M}_0)}{4\pi} \right] \mathrm{d}^3\mathbf{r}. \tag{4}$$

It can be seen that the magnetization $\mathbf{M}_0$ acts as an external field, which leads to the emergence of a spontaneous mixed state in ferromagnetic superconductors with the vortices directed along $\mathbf{M}_0$. This situation is not very interesting, since the spatial dispersion does not matter when the magnetic field is parallel to $\mathbf{M}_0$. The influence of the spontaneous magnetization can be compensated by an external field directed in the $-x$-direction. If the sample has a vanishing demagnetizing factor N_{xx}, the compensating field simply equals $-4\pi\mathbf{M}_0$ (if $N_{xx} \neq 0$, this field is somewhat smaller). If we substitute $\mathbf{H}_e = -4\pi\mathbf{M}_0$ into eq. (4), we may see that in equilibrium the field component B_x should be of the order of or smaller than m^2/M, hence, the term containing $B_x m^2$ is much smaller than m^2, and it can be neglected. Hence, at $\mathbf{H}_e = -4\pi\mathbf{M}_0$ eq. (4) reduces to eq. (2). Thus, the formalism developed below can be applied to both SF superlattices and ferromagnetic superconductors.

The vortex state. – Minimizing F with respect to $\mathbf{m}$ and $\mathbf{a}$, we obtain the following relations for the Fourier transforms:

$$\mathbf{m}(\mathbf{q}) = (K + \alpha q^2)^{-1}\mathbf{B}(\mathbf{q}), \tag{5}$$

$$i\mathbf{q} \times \mathbf{B}(\mathbf{q}) = -\frac{1}{\lambda^2}\mu_{zz}(q)\left[\mathbf{A}(\mathbf{q}) + \frac{\Phi_0}{2\pi}\nabla\theta(\mathbf{q})\right], \tag{6}$$

where $\mathbf{q}$ is the 2D wave vector in the Fourier space, and $\mu_{zz}(q) = 1 + 4\pi(K - 4\pi + \alpha q^2)^{-1}$ is the permeability in the z-direction. The second term in the expression for μ_{zz} is responsible for the nonlocal electrodynamics generated by the magnetic subsystem.

Now we may calculate the vortex field profile, $B_z(\rho)$ (ρ is the distance from the vortex axis), using eq. (6) and the relations

$$i\mathbf{q} \times \mathbf{A}(\mathbf{q}) = \mathbf{B}(\mathbf{q}), \qquad \nabla\theta(\mathbf{q}) = i\frac{\mathbf{z}_0 \times \mathbf{q}}{2\pi q^2},$$

where $\mathbf{z}_0$ is a unit vector directed along the z-axis. The Fourier transform of $B_z(\rho)$ can be presented in the form

$$B_z(\mathbf{q}) = \frac{\Phi_0}{4\pi^2\lambda^2 L^2(q_2^2 - q_1^2)}\left[\frac{1 - L^2q_1^2}{q^2 + q_1^2} - \frac{1 - L^2q_2^2}{q^2 + q_2^2}\right], \tag{7}$$

where

$$q_{1,2}^2 = \frac{L^2 + \tilde{\lambda}^2 \pm \sqrt{(L^2 + \tilde{\lambda}^2)^2 - 4L^2\lambda^2}}{2L^2\lambda^2}, \tag{8}$$

$\tilde{\lambda} = \lambda\mu_{zz}^{-1/2}(0)$ is the renormalized London penetration depth [13], and $L = (\alpha/K)^{1/2}$ is the magnetic nonlocality scale. The inverse Fourier transform of eq. (7) is straightforward, and one immediately obtains

$$B_z = \frac{\Phi_0}{2\pi\lambda^2 L^2(q_2^2 - q_1^2)}\Big[\left(1 - L^2q_1^2\right)\mathrm{K}_0(q_1\rho) - \left(1 - L^2q_2^2\right)\mathrm{K}_0(q_2\rho)\Big], \tag{9}$$

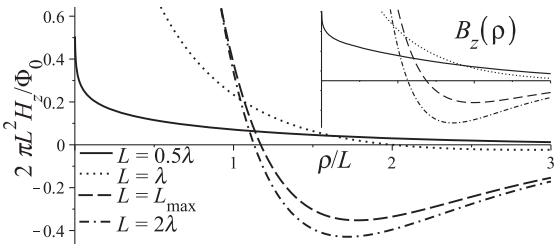

Fig. 2: The H-field profiles of a single vortex at $\mu_{zz}(0) = 5$ and different ratios L/λ. Inset: the profiles of B_z, in arbitrary units.

where K_0 is the modified Bessel function and $\mathrm{Re}(q_{1,2}) > 0$. The H-field, defined as $H_z = B_z - 4\pi m_z$ or $H_z(\mathbf{q}) = \mu_{zz}^{-1}(q)B_z(\mathbf{q})$, can be calculated in a similar way:

$$H_z = \frac{\Phi_0}{2\pi\lambda^2 L^2(q_2^2 - q_1^2)}\Big[\left(1 - 4\pi K^{-1} - L^2q_1^2\right)\mathrm{K}_0(q_1\rho) - \left(1 - 4\pi K^{-1} - L^2q_2^2\right)\mathrm{K}_0(q_2\rho)\Big]. \tag{10}$$

It is remarkable that the quantities q_1 and q_2 become complex when $L_{\min} < L < L_{\max}$, where

$$L_{\min,\max} = \lambda\left[1 \mp \sqrt{\frac{4\pi}{K}}\right] = \lambda\left[1 \mp \sqrt{\frac{\mu_{zz}(0) - 1}{\mu_{zz}(0)}}\right]. \tag{11}$$

Then, $B_z(\rho)$ and $H_z(\rho)$ exhibit damped spatial oscillations. The situation formally resembles the behavior predicted by Eilenberger [17] and Dichtel [18] for low-κ superconductors. However, at $L > L_{\max}$ the oscillations disappear: the fields change their sign once, remaining negative at $\rho \to \infty$. Some graphs of the magnetic induction $B_z(\rho)$ and of the H-field are shown in fig. 2.

Taking a sample with a vanishing demagnetizing factor N_{zz} and using eqs. (2), (5) and (6) one can obtain $F = \int \boldsymbol{\kappa}\mathbf{H}\mathrm{d}^3\mathbf{r}/8\pi$, where $\boldsymbol{\kappa} = -\Phi_0\,\mathrm{rot}\,\nabla\theta/(2\pi)$ is the vorticity, and $\mathbf{H} = \mathbf{B} - 4\pi\mathbf{m}$. Thus, for $L > L_{\min}$, *i.e.*, for

$$L > \lambda_0\sqrt{\frac{d}{d_S}}\left[1 - \sqrt{\frac{\mu_{zz}(0) - 1}{\mu_{zz}(0)}}\right], \tag{12}$$

the sign change of $H_z(\rho)$ results in the attraction of vortices. Here the length $L \simeq L_0 = \sqrt{\alpha_0/K_0}$ coincides with the Bloch domain wall width of the ferromagnetic layers [19] (note that we do not consider systems containing domains, so L_0 is just a characteristic length scale). In our case the unusual behavior of the vortex field is a consequence of the strong spatial dispersion of $\mu_{zz}(q)$, unlike in refs. [4–8], where the sign reversal appeared due to the anisotropy. In ref. [20] it has been erroneously claimed that a large value of μ_{zz} is sufficient for the attraction of vortices, so that the dispersion is not required. Indeed, if we put $\alpha = 0$ in μ_{zz} we obtain a well-known renormalization of λ in eq. (6), which does not lead to any field reversal [13]. Still, the numerical simulations presented in ref. [20] revealed the clusterization of vortices, apparently

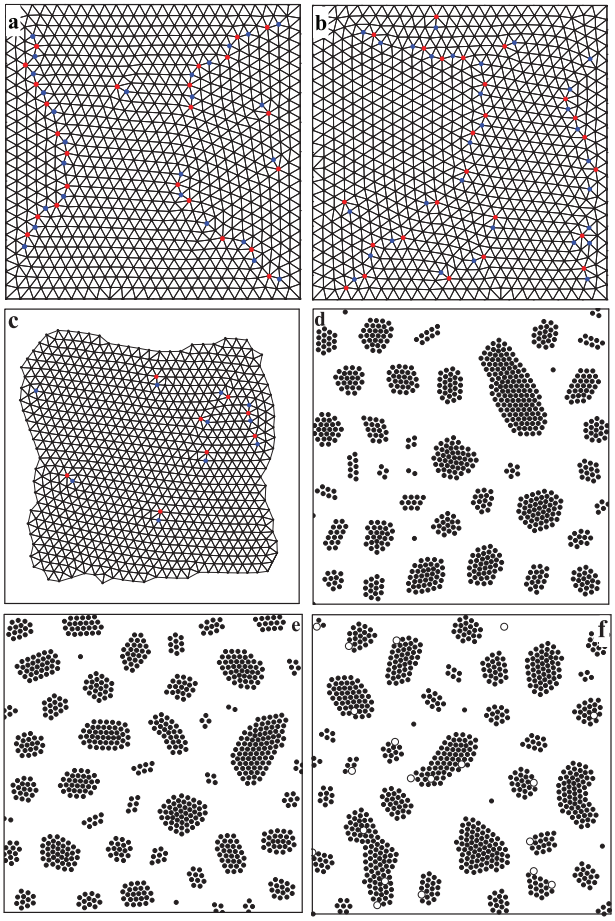

Fig. 3: (Colour on-line) (a)–(c) Delaunay triangulations of vortex configurations in a ferromagnetic superconductor or SF superlattice with the parameters $\mu_{zz}(0) \gg 1$ and $L\mu_{zz}(0)/\lambda = 2$. The size of the box is (a) $50\lambda' \times 50\lambda'$, (b) $60\lambda' \times 60\lambda'$, and (c) $90\lambda' \times 90\lambda'$, where $\lambda' = \sqrt{L\lambda}$. The fivefold- and sevenfold-coordinated vortices, forming lattice dislocations, are marked as blue and red points, respectively. (d), (e): two realizations of a metastable state with different (random) initial conditions. The dots denote vortices. (f) Metastable configuration with 20 pinned (fixed) vortices, marked as hollow circles. In (d)–(f) the size of the box is $150\lambda' \times 150\lambda'$.

connected with the dispersion of the permeability, which has been actually included in the model. This fact is in good accordance with our analysis.

To determine the equilibrium vortex configurations in our system we modelled numerically the relaxation to equilibrium of 800 vortices confined in a box with rigid walls. The relaxation process was goverened by the equations

$$\eta \frac{\mathrm{d}\mathbf{R}_i}{\mathrm{d}t} = -\frac{\partial F}{\partial \mathbf{R}_i}, \tag{13}$$

where $\mathbf{R}_i$ is the position of the i-th vortex, and $\eta > 0$ is a viscosity coefficient. This algorithm allows to find a local minimum of the free energy. The relaxation was stopped when all derivatives $\mathrm{d}\mathbf{R}_i/\mathrm{d}t$ became sufficiently small. Some final vortex configurations are shown in fig. 3. The parameters K, L and λ were chosen so that the vortex

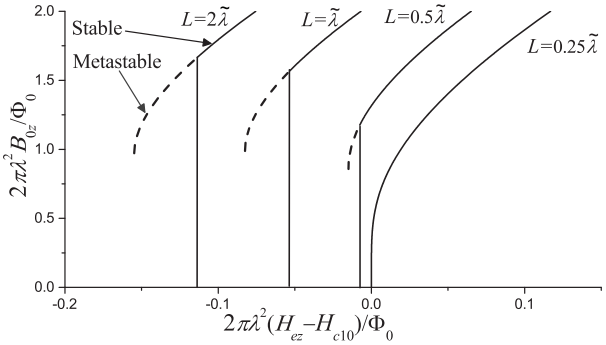

Fig. 4: The B_{0z}-*vs.*-H_{ez} dependences at low fields ($H_{ez} \ll H_{c2}$) and $\mu_{zz}(0) = 4$ ($L_{\min} = 0.268\tilde{\lambda}$) plotted for different ratios $L/\tilde{\lambda}$.

field oscillations were present. In this respect our calculations differ from those given in refs. [21–23], where a nonoscillating attractive potential was used to study the vortex structures in superconductors with competing attractive and repulsive vortex interaction. Generally, we observed either a uniform hexagonal vortex state with several defects (fig. 3(a) and (b)) or vortex clusters with a regular internal hexagonal structure (fig. 3(c)–(f)). No traces of square configurations were found. Relying on this observation, we calculated the magnetization curves of the ferromagnetic superconductor with $N_{zz} = 0$, assuming that the lattice is triangular. The z-component of the internal field, B_{0z}, satisfies the relation $H_{ez} = 4\pi V^{-1} \partial F/\partial B_{0z}$, where $\mathbf{H}_e$ is an applied external field, and V is the sample volume. Several B_{0z}-*vs.*-H_{ez} curves for different temperatures T are shown in fig. 4. At high temperatures, when λ is large as compared to L, the B_{0z}-*vs.*-H_{ez} dependence is smooth, like in ordinary type-II superconductors. At lower temperatures, when $L > L_{\min}$ and the long-ranged vortex-vortex attraction appears, the curves exhibit a jump of the internal field, corresponding to a first-order phase transition at $H_{ez} = H_{c1}$. The lower critical field H_{c1} is determined from the condition of equality of the thermodynamic potential at a zero internal field and the thermodynamic potential in the presence of vortices. The attractive interaction of vortices results in H_{c1} being somewhat smaller than the classical lower critical field H_{c10}, defined by the energy of an isolated flux line [24]. When the phase transition at H_{c1} is of the first order, the vortex phase may be "overcooled": when lowering the external field below H_{c1} one may still have vortices. The metastable overcooling branches of the B_{0z}-*vs.*-H_{ez} curves are shown in fig. 4 as dashed lines. Thus, when measuring the magnetization curves of the SF system one should expect hysteretic behavior in the vicinity of $H_{ez} = H_{c1}$.

Experimentally, vortex structures are usually observed in films with the external field applied perpendicularly to the film. In this geometry $N_{zz} \approx 4\pi$, and $B_{0z} \approx H_{ez}$, so that the average vortex density is fixed. In a SF superlattice of a finite thickness $l_z \gg \lambda$, the vortex-vortex interaction remains attractive at intermediate distances,

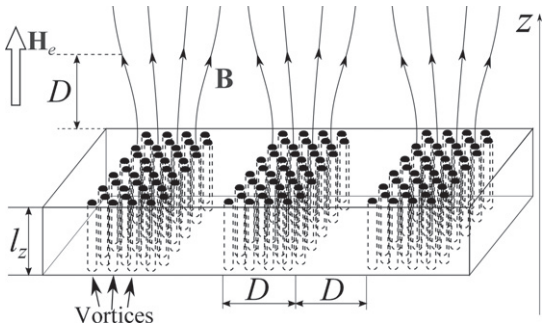

Fig. 5: A schematic picture of the stripe domain structure in the intermediate mixed state of the SF system at $H_{ez} \approx B_{0z}(H_{c1})/2$.

acquiring a long-range repulsive tail due to the unscreened magnetostatic interaction through the free space. Then, an intermediate mixed state with coexisting vortex and Meissner phase domains should occur [3]. The equilibrium magnetic field in the vortex phase domains equals to the value $B_{0z}(H_{c1})$ obtained by minimizing the free energy per vortex.

To estimate the characteristic size D of the vortex domains we will assume that the pattern has a stripe structure, as shown in fig. 5. Let us consider the free energy F_a per unit area of the film at $H_{ez} \approx B_{0z}(H_{c1})/2$, when a half of the sample is in the mixed state. The contribution to F_a from the mixed/Meissner state interfaces equals $\sigma l_z/D$, where σ is the surface tension energy per unit area of the interface. Another contribution to F_a originates from the magnetostatic energy concentrated in the regions with a thickness of the order of D above and below the film, where the magnetic field is considerably inhomogeneous. Thus,

$$F_a = \tilde{C}(D)B_{0z}^2(H_{c1})D + \sigma l_z/D + \text{const}, \qquad (14)$$

where $\tilde{C}(D)$ is a function of the order of unity, weakly depending on D. The minimization of F_a with respect to D yields $D \propto \sqrt{l_z}$, which resembles the behavior of the size of magnetic domains in a ferromagnetic slab [25]. This estimate is valid when D is much larger than the intervortex distance: $D \gg \sqrt{\Phi_0/B_{0z}(H_{c1})}$.

Considering optimal SF superlattices needed to observe the above effects experimentally, one should choose, of course, the ferromagnetic layer material with a large domain wall width L_0 (according to the condition (12)), such as yttrium iron garnet [26] or permalloy [27], both having $L_0 \gtrsim 100\,\text{nm}$. Indeed, a pretty weak magnetic anisotropy in the yttrium iron garnet samples can result in the domain wall width L_0 of the order of 1–2 μm size [28]. It is also important that in this material the value $\mu_{zz}(0) \sim$2–3 [29] responsible for the renormalization of the London penetration depth is rather large to weaken the restrictions on the L_0 scale. Superconducting layers can be prepared, *e.g.*, from lead or niobium ($\lambda_0 \lesssim 100\,\text{nm}$). The latter typically has a large parameter κ due to impurities, when prepared as a thin film [30].

Recently, a lot of attention has been given to the $YBa_2Cu_3O_7/La_{1-x}Ca_xMnO_3$ (YBCO/LCMO) superlattices (see, *e.g.*, [31] and references cited therein). It is remarkable that such systems also allow to obtain negative refraction [32]. Unfortunately, the thickness of the domain wall of LCMO $L_0 \sim 12\,\text{nm}$ [33] is smaller than the London penetration depth in YBCO and the magnetic permeability of the LCMO layers $\mu_{zz}(0) \sim$3–4 [34] is not large enough to satisfy the condition (12) easily. Such parameters make the observation of the clustering effect in these systems rather improbable. Among the promising candidates it is worth mentioning the superlattice NbSe2/Py [35] where the relation of the above characteristic lengths is more reasonable: $L_0 \sim 210\,\text{nm}$ and $\lambda \sim 130\,\text{nm}$.

As mentioned above, our analysis may be also fully applied to ferromagnetic superconductors. However, the U-based ferromagnetic superconductors UGe2 [14], URhGe [15] and UCoGe [16] reveal a strong magnetic anisotropy and weak magnetic susceptibility. Therefore, the intervortex interaction in these compounds should be repulsive, as usual. The compound $ErRh_4B_4$ [36] seems to be a type-I superconductor with a strongly nonuniform magnetic structure in the phase where ferromagnetism and superconductivity coexist. Another candidate, the weak ferromagnet $ErNi_2B_2C$ [37], has a relatively small value of $\lambda \approx 70\,\text{nm}$ [38] and the Curie temperature well below the superconducting transition temperature. As a result, measurements of the magnetic permeability are hampered by the Meissner effect, and corresponding data are not available to date.

Conclusion. – We have demonstrated that the nonlocal electrodynamics in high-κ SF superlattices leads to the attraction of Abrikosov vortices. At sufficiently low temperatures these structures may exhibit the transition to a very unusual type of the vortex state characterized by an oscillating vortex field, a first-order phase transition at H_{c1} and formation of an intermediate mixed state. Besides the obvious peculiarities of the magnetization curves one can expect that the state with vortex stripes could reveal strongly anisotropic pinning and resistivity in the flux-flow regime. An important feature of the SF multilayer system is its high tunability: the phase diagram can be engineered by choosing different materials and layer thicknesses d_S and d_F. The superlattice revealing the predicted unusual superconducting electrodynamics may be fabricated on the basis of yttrium iron garnet magnetic layers and niobium or lead superconducting layers.

* * *

We are grateful to L. Bulaevskii, J. Villegas and V. K. Vlasko-Vlasov for useful discussions. This work was supported in part by the Russian Foundation for Basic Research, the French ANR program electroVortex, LabEx Amadeus program, NanoSC COST Action No. MP1201,

and the grant of the Russian Ministry of Science and Education No. 02.B.49.21.0003.

REFERENCES

[1] Leung M., *J. Low Temp. Phys.*, **12** (1973) 215.
[2] Auer J. and Ullmaier H., *Phys. Rev. B*, **7** (1973) 136.
[3] Brandt E. H. and Das M. P., *J. Supercond. Nov. Magn.*, **24** (2011) 57.
[4] Buzdin A. I. and Simonov A. Y., *JETP Lett.*, **51** (1990) 191.
[5] Kogan V. G., Nakagawa N. and Thiemann S. L., *Phys. Rev. B*, **42** (1990) 2631.
[6] Grishin A. M., Martinovich A. Y. and Yampol'skiy S. V., *Sov. Phys. JETP*, **70** (1990) 1089.
[7] Buzdin A. and Simonov A., *Physica C*, **175** (1991) 143.
[8] Buzdin A., Krotov S. and Kuptsov D., *Physica C: Supercond.*, **175** (1991) 42.
[9] Bending S. J. and Dodgson M. J. W., *J. Phys.: Condens. Matter*, **17** (2005) R955.
[10] Uribe-Laverde M. A., Satapathy D. K., Marozau I., Malik V. K., Das S., Sen K., Stahn J., Rühm A., Kim J.-H., Keller T., Devishvili A., Toperverg B. P. and Bernhard C., *Phys. Rev. B*, **87** (2013) 115105.
[11] Dybko K., Aleshkevych P., Sawicki M., Paszkowicz W. and Przyslupski P., *J. Phys.: Condens. Matter*, **25** (2013) 376001.
[12] Buzdin A. I., *Rev. Mod. Phys.*, **77** (2005) 935.
[13] Bulaevskii L., Buzdin A., Kulić M. and Panjukov S., *Adv. Phys.*, **34** (1985) 175.
[14] Saxena S. S., Agarwal P., Ahilan K., Grosche F. M., Haselwimmer R. K. W., Steiner M. J., Pugh E., Walker I. R., Julian S. R., Monthoux P., Lonzarich G. G., Huxley A., Sheikin I., Braithwaite D. and Flouquet J., *Nature*, **406** (2000) 587.
[15] Aoki D., Huxley A., Ressouche E., Braithwaite D., Flouquet J., Brison J.-P., Lhotel E. and Paulsen C., *Nature*, **413** (2001) 613.
[16] Huy N. T., Gasparini A., de Nijs D. E., Huang Y., Klaasse J. C. P., Gortenmulder T., de Visser A., Hamann A., Görlach T. and Löhneysen H. v., *Phys. Rev. Lett.*, **99** (2007) 067006.
[17] Eilenberger G. and Büttner H., *Z. Phys.*, **224** (1969) 335.
[18] Dichtel K., *Phys. Lett. A*, **35** (1971) 285.
[19] Kittel C., *Introduction to Solid State Physics*, 8th edition (Wiley, NJ) 2004.
[20] Lin S.-Z., Bulaevskii L. N. and Batista C. D., *Phys. Rev. B*, **86** (2012) 180506.
[21] Xu X. B., Fangohr H., Wang Z. H., Gu M., Liu S. L., Shi D. Q. and Dou S. X., *Phys. Rev. B*, **84** (2011) 014515.
[22] Zhao H. J., Misko V. R. and Peeters F. M., *New J. Phys.*, **14** (2012) 063032.
[23] Reichhardt C., Drocco J., Olson Reichhardt C. and Bishop A., *J. Supercond. Nov. Magn.*, **26** (2013) 2041.
[24] Tinkham M., *Introduction to Superconductivity*, second edition, *Dover Books on Physics Series* (Dover Publications) 2004.
[25] Landau L. D., Pitaevskii L. P. and Lifshitz E. M., *Electrodynamics of Continuous Media*, Vol. **8**, *Course of Theoretical Physics*, 2nd edition (Butterworth-Heinemann, Oxford) 1984.
[26] Koronovskyy V. E., *Funct. Mater.*, **13** (2006) 515.
[27] Trunk T., Redjdal M., Kákay A., Ruane M. F. and Humphrey F. B., *J. Appl. Phys.*, **89** (2001) 7606.
[28] Vlasko-Vlasov V. K., Dedukh L. M. and Nikitenko V. I., *Sov. Phys. JETP*, **44** (1976) 1208.
[29] Popova E., Keller N., Gendron F., Guyot M., Brianso M.-C., Dumond Y. and Tessier M., *J. Appl. Phys.*, **90** (2001) 1422.
[30] Gubin A. I., Il'in K. S., Vitusevich S. A., Siegel M. and Klein N., *Phys. Rev. B*, **72** (2005) 064503.
[31] Das S., Sen K., Marozau I., Uribe-Laverde M. A., Biskup N., Varela M., Khaydukov Y., Soltwedel O., Keller T., Döbeli M., Schneider C. W. and Bernhard C., *Phys. Rev. B*, **89** (2014) 094511.
[32] Pimenov A., Loidl A., Przyslupski P. and Dabrowski B., *Phys. Rev. Lett.*, **95** (2005) 247009.
[33] Lloyd S. J., Mathur N. D., Loudon J. C. and Midgley P. A., *Phys. Rev. B*, **64** (2001) 172407.
[34] Nemes N., Garcia-Hernandez M., Szatmari Z., Feher T., Simon F., Visani C., Pena V., Miller C., Garcia-Barriocanal J., Bruno F., Sefrioui Z., Leon C. and Santamaria J., *IEEE Trans. Magn.*, **44** (2008) 2926.
[35] Vlasko-Vlasov V., Welp U., Karapetrov G., Novosad V., Rosenmann D., Iavarone M., Belkin A. and Kwok W.-K., *Phys. Rev. B*, **77** (2008) 134518.
[36] Prozorov R., Vanette M. D., Law S. A., Bud'ko S. L. and Canfield P. C., *Phys. Rev. B*, **77** (2008) 100503.
[37] Galvis J. A., Crespo M., Guillamón I., Suderow H., Vieira S., García Hernández M., Bud'ko S. and Canfield P. C., *Solid State Commun.*, **152** (2012) 1076.
[38] Canfield P. C., Kogan V. G., Eskildsen M. R., Andersen N. H., Mortensen K. and Harada K., *Phys. Rev. Lett.*, **82** (1999) 1756.